

# QUARKONIUM PRODUCTION AT THE EIC: UNPOLARISED-NUCLEON PDF FROM $J/\psi$ & $\Upsilon$ PRODUCTION

**Yelyzaveta Yedelkina**

Jan 10, 2022

QaT2022, Aussois  
Jan 9-15, 2022



This project is supported by the European Union's Horizon 2020 research and innovation programme under Grant agreement no. 824093

# Part I

## Introducing inclusive $J/\psi$ & $\Upsilon$ photoproduction

# Introduction: inclusive $J/\psi(Y)$ photoproduction

C.-H. Chang, NPB172, 425 (1980); R. Baier & R. Rückl Z. Phys. C 19, 251(1983);

Let's us first discuss **inclusive  $J/\psi(Y)$  photoproduction**:

- as a reminder,  $J/\psi(Y)$  is a  $c\bar{c}$  ( $b\bar{b}$ ) bound state with  $J = 1$ ,  $L = 0$ ,  $S = 1$ ; **vector** particle
- **inclusive photoproduction**:

$$\gamma(Q^2 \simeq 0) + p \rightarrow J/\psi + X;$$

- We will discuss the photoproduction at **NLO**;

# Introduction: inclusive $J/\psi(\Upsilon)$ photoproduction

C.-H. Chang, NPB172, 425 (1980); R. Baier & R. Rückl Z. Phys. C 19, 251(1983);

Let's us first discuss **inclusive  $J/\psi(\Upsilon)$  photoproduction**:

- as a reminder,  $J/\psi(\Upsilon)$  is a  $c\bar{c}$  ( $b\bar{b}$ ) bound state with  $J = 1$ ,  $L = 0$ ,  $S = 1$ ; **vector** particle
- **inclusive photoproduction**:

$$\gamma(Q^2 \simeq 0) + p \rightarrow J/\psi + X;$$

- We will discuss the photoproduction at **NLO**;
- **3 common models** (differences in the treatment of the hadronisation):
  - ▶ **Colour Singlet Model**;
  - ▶ NRQCD and Colour Octet Mechanism;
  - ▶ Colour Evaporation Model;

# Introduction: inclusive $J/\psi(\Upsilon)$ photoproduction

C.-H. Chang, NPB172, 425 (1980); R. Baier & R. Rückl Z. Phys. C 19, 251(1983);

Let's us first discuss **inclusive  $J/\psi(\Upsilon)$  photoproduction**:

- as a reminder,  $J/\psi(\Upsilon)$  is a  $c\bar{c}$  ( $b\bar{b}$ ) bound state with  $J = 1$ ,  $L = 0$ ,  $S = 1$ ; **vector** particle
- **inclusive photoproduction**:

$$\gamma(Q^2 \simeq 0) + p \rightarrow J/\psi + X;$$

- We will discuss the photoproduction at **NLO**;
- **3 common models** (differences in the treatment of the hadronisation):
  - ▶ **Colour Singlet Model**;
  - ▶ NRQCD and Colour Octet Mechanism;
  - ▶ Colour Evaporation Model;
- We do not discuss large  $z$  and exclusive reactions

→ see the exclusive sessions

# Resolved-photon contributions

J.P. Lansberg, Phys.Rept. 889 (2020)

- At high energies, the hadronic content of the photon can be 'resolved' during the collisions
- Are very similar to those for hadroproduction

# Resolved-photon contributions

J.P. Lansberg, Phys.Rept. 889 (2020)

- At high energies, the hadronic content of the photon can be 'resolved' during the collisions
- Are very similar to those for hadroproduction
- At low  $z$  they can appear as important where only a small fraction of the photon energy is involved in the quarkonium production (limited impact at HERA)
- At lower energies, like at the EIC, their impact should be further reduced
- Can be avoided by a simple kinematical cut on low elasticity values,  $z$

# Resolved-photon contributions

J.P. Lansberg, Phys.Rept. 889 (2020)

- At high energies, the hadronic content of the photon can be 'resolved' during the collisions
- Are very similar to those for hadroproduction
- At low  $z$  they can appear as important where only a small fraction of the photon energy is involved in the quarkonium production (limited impact at HERA)
- At lower energies, like at the EIC, their impact should be further reduced
- Can be avoided by a simple kinematical cut on low elasticity values,  $z$
- It will be needed to re-evaluate its impact → as M. Rinaldi will discuss



# General structure of NLO corrections

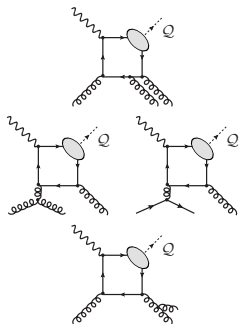
Singularities at NLO [and how they are removed]:

# General structure of NLO corrections

Singularities at NLO [and how they are removed]:

- Real emission

- ▶ Infrared divergences: Soft [cancelled by loop IR contr. after phase-space integration (the KLN theorem)]
- ▶ Infrared divergences: Collinear



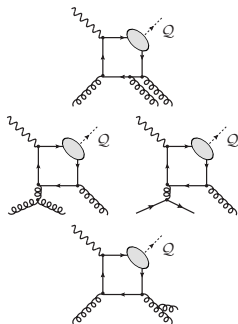
[The quark and antiquark attached to the ellipsis are taken as on-shell and their relative velocity  $v$  is set to zero.]

# General structure of NLO corrections

Singularities at NLO [and how they are removed]:

- Real emission

- ▶ Infrared divergences: Soft [cancelled by loop IR contr. after phase-space integration (the KLN theorem)]
- ▶ Infrared divergences: Collinear
  - ★ initial emission [subtracted by Altarelli-Parisi counter-terms (AP-CT) in the factorised PDFs]
  - ★ final emission [cancelled by loop Infrared contribution after phase-space integration (the KLN theorem)]



[The quark and antiquark attached to the ellipsis are taken as on-shell and their relative velocity  $v$  is set to zero.]

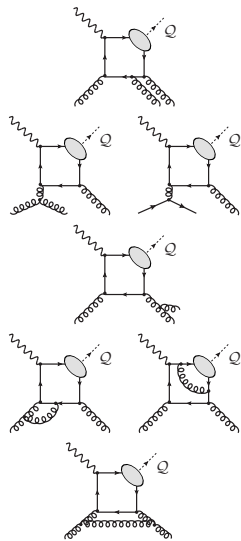
# General structure of NLO corrections

Singularities at NLO [and how they are removed]:

- Real emission

- ▶ Infrared divergences: Soft [cancelled by loop IR contr. after phase-space integration (the KLN theorem)]
- ▶ Infrared divergences: Collinear
  - ★ initial emission [subtracted by Altarelli-Parisi counter-terms (AP-CT) in the factorised PDFs]
  - ★ final emission [cancelled by loop Infrared contribution after phase-space integration (the KLN theorem)]

- Virtual (loop) contribution



[The quark and antiquark attached to the ellipsis are taken as on-shell and their relative velocity  $v$  is set to zero.]

# General structure of NLO corrections

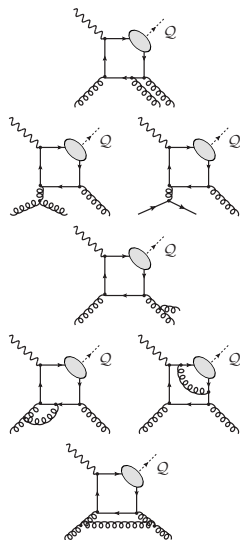
Singularities at NLO [and how they are removed]:

- **Real emission**

- ▶ **Infrared divergences: Soft** [cancelled by loop IR contr. after phase-space integration (the KLN theorem)]
- ▶ **Infrared divergences: Collinear**
  - ★ **initial emission** [subtracted by Altarelli-Parisi counter-terms (AP-CT) in the factorised PDFs]
  - ★ **final emission** [cancelled by loop Infrared contribution after phase-space integration (the KLN theorem)]

- **Virtual (loop) contribution**

- ▶ **Ultraviolet divergences:** [removed by renormalisation]
- ▶ **Infrared divergences:** [cancelled by real Infrared contribution]



[The quark and antiquark attached to the ellipsis are taken as on-shell and their relative velocity  $v$  is set to zero.]

## Part II

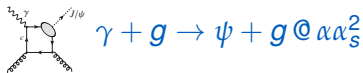
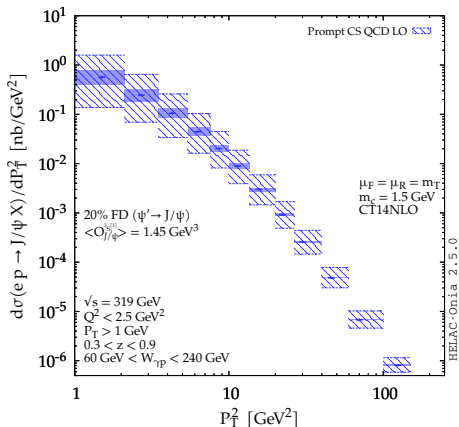
# Photoproduction at mid and high $P_T$ at HERA

# Different contributions in the CSM up to NLO

C.Flore, JP Lansberg, H.S. Shao, YY, PLB 811 (2020) 135926

# Different contributions in the CSM up to NLO

C.Flore, JP Lansberg, H.S. Shao, YY, PLB 811 (2020) 135926



## Notes:

All the computations were done with HELAC-ONIA. The scale and mass uncertainties are shown by the hatched and solid bands.

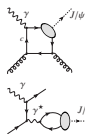
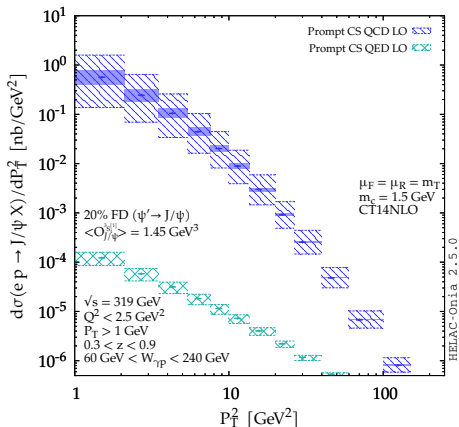
**H.S. Shao, CPC198 (2016) 238**; See also <https://nloaccess.in2p3.fr>

[The quark and antiquark attached to the ellipsis are taken as on-shell and their relative velocity  $v$  is set to zero.]



# Different contributions in the CSM up to NLO

C.Flore, JP Lansberg, H.S. Shao, YY, PLB 811 (2020) 135926



$$\gamma + g \rightarrow \psi + g @ \alpha \alpha_s^2$$

$$\gamma + q \rightarrow \psi + q @ \alpha^3 \text{ [NEW !]}$$

Notes:

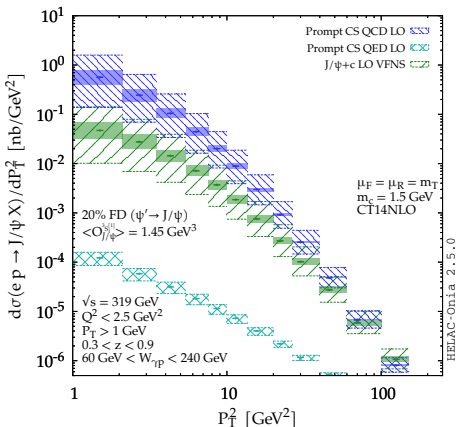
All the computations were done with HELAC-ONIA. The scale and mass uncertainties are shown by the hatched and solid bands.

**H.S. Shao, CPC198 (2016) 238**; See also <https://nloaccess.in2p3.fr>

[The quark and antiquark attached to the ellipsis are taken as on-shell and their relative velocity  $v$  is set to zero.]

# Different contributions in the CSM up to NLO

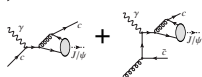
C.Flore, JP Lansberg, H.S. Shao, YY, PLB 811 (2020) 135926



$$\gamma + g \rightarrow \psi + g @ \alpha \alpha_s^2$$



$$\gamma + q \rightarrow \psi + q @ \alpha^3 \text{ [NEW !]}$$



$$\left\{ \begin{array}{l} \gamma + c \rightarrow \psi + c @ \alpha \alpha_s^2 \text{ w. 4 Flavour Scheme} \\ \gamma + g \rightarrow \psi + c + \bar{c} @ \alpha \alpha_s^3 \text{ w. 3 Flavour Scheme} \end{array} \right. \text{VFNS [also NEW !]}$$

Notes:

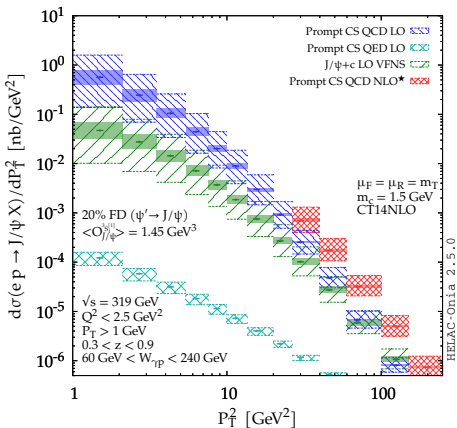
All the computations were done with HELAC-ONIA. The scale and mass uncertainties are shown by the hatched and solid bands.

**H.S. Shao, CPC198 (2016) 238**; See also <https://nloaccess.in2p3.fr>

[The quark and antiquark attached to the ellipsis are taken as on-shell and their relative velocity  $v$  is set to zero.]

# Different contributions in the CSM up to NLO

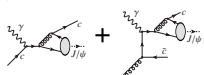
C.Flore, JP Lansberg, H.S. Shao, YY, PLB 811 (2020) 135926



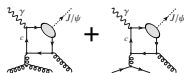
$$\gamma + g \rightarrow \psi + g @ \alpha \alpha_s^2$$



$$\gamma + q \rightarrow \psi + q @ \alpha^3 \text{ [NEW !]}$$



$$\left\{ \begin{array}{l} \gamma + c \rightarrow \psi + c @ \alpha \alpha_s^2 \text{ w. 4 Flavour Scheme} \\ \gamma + g \rightarrow \psi + c + \bar{c} @ \alpha \alpha_s^3 \text{ w. 3 Flavour Scheme} \end{array} \right. \text{VFNS [also NEW !]}$$



$$\left\{ \begin{array}{l} \gamma + g \rightarrow \psi + g + g @ \alpha \alpha_s^3 \\ \gamma + q \rightarrow \psi + g + q @ \alpha \alpha_s^3 \end{array} \right.$$

$$[+ \gamma + g \rightarrow \psi + g]$$

Notes:

All the computations were done with HELAC-ONIA. The scale and mass uncertainties are shown by the hatched and solid bands.

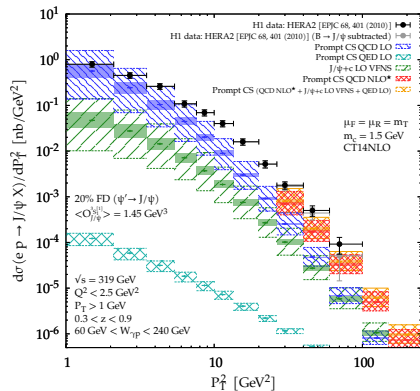
H.S. Shao, CPC198 (2016) 238; See also <https://nloaccess.in2p3.fr>

[The quark and antiquark attached to the ellipsis are taken as on-shell and their relative velocity  $v$  is set to zero.]

NLO\* only contains the real-emission contributions with an IR cut-off and is expected to account for the leading  $P_T$  contributions at NLO ( $P_T^{-6}$ ). It has been successfully checked against full NLO computations for  $P_T > 3 \text{ GeV}$ .

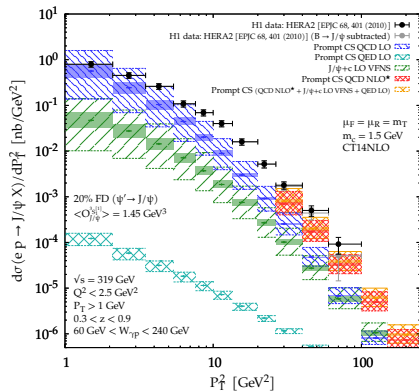
# Comparison to the latest HERA data by H1

C.Flore, JP Lansberg, H.S. Shao, YY, PLB 811 (2020) 135926



# Comparison to the latest HERA data by H1

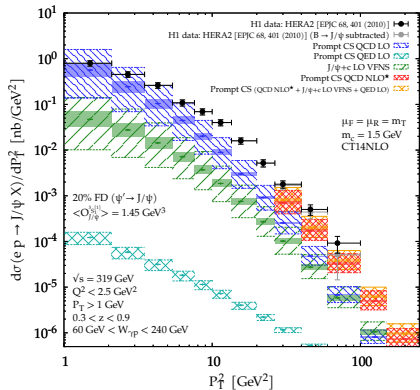
C.Flore, JP Lansberg, H.S. Shao, YY, PLB 811 (2020) 135926



- LO QCD : OK at low  $P_T$

# Comparison to the latest HERA data by H1

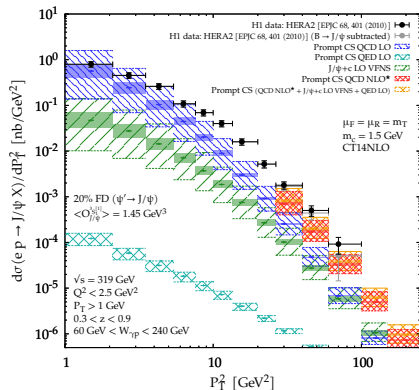
C.Flore, JP Lansberg, H.S. Shao, YY, PLB 811 (2020) 135926



- LO QCD : OK at low  $P_T$
- LO QED small but much harder

# Comparison to the latest HERA data by H1

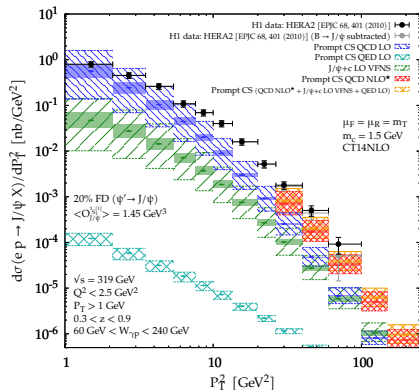
C.Flore, JP Lansberg, H.S. Shao, YY, PLB 811 (2020) 135926



- LO QCD : OK at low  $P_T$
- LO QED small but much harder
- $J/\psi$ +charm: matter at high  $P_T$

# Comparison to the latest HERA data by H1

C.Flore, JP Lansberg, H.S. Shao, YY, PLB 811 (2020) 135926

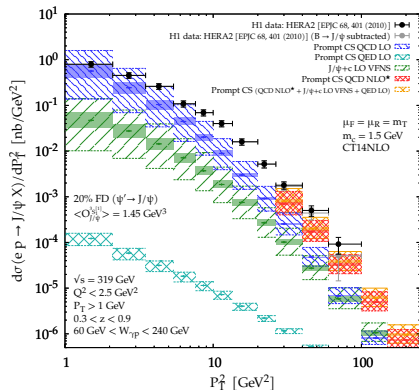


- LO QCD : OK at low  $P_T$
- LO QED small but much harder
- $J/\psi$ +charm: matter at high  $P_T$
- NLO(\*) close the data, the overall sum nearly agrees with them



# Comparison to the latest HERA data by H1

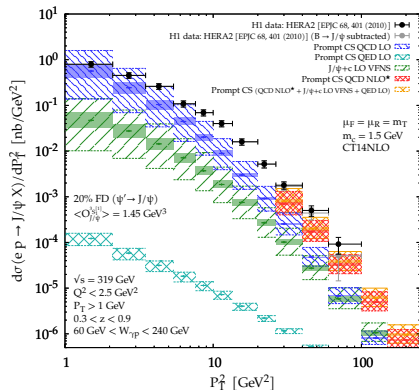
C.Flore, JP Lansberg, H.S. Shao, YY, PLB 811 (2020) 135926



- LO QCD : OK at low  $P_T$
- LO QED small but much harder
- $J/\psi$ +charm: matter at high  $P_T$
- NLO(\*) close the data, the overall sum nearly agrees with them
- Agreement with the last bin when the expected  $B \rightarrow J/\psi$  feed down (in gray) is subtracted

# Comparison to the latest HERA data by H1

C.Flore, JP Lansberg, H.S. Shao, YY, PLB 811 (2020) 135926



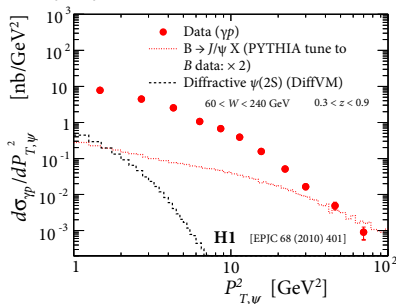
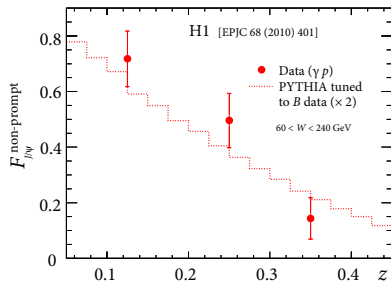
- LO QCD : OK at low  $P_T$
- LO QED small but much harder
- $J/\psi$ +charm: matter at high  $P_T$
- NLO(\*) close the data, the overall sum nearly agrees with them
- Agreement with the last bin when the expected  $B \rightarrow J/\psi$  feed down (in gray) is subtracted

The CSM up to  $\alpha\alpha_s^3$  reproduces photoproduction at HERA

→ the EIC predictions can rely on CSM only

# Feed down

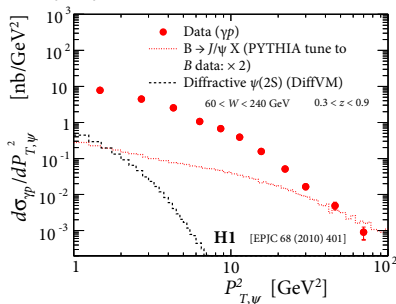
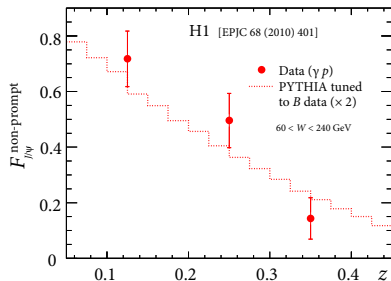
J.P. Lansberg, Phys.Rept. 889 (2020); C.Flore, JP Lansberg, H.S. Shao, YY, PLB 811 (2020) 135926



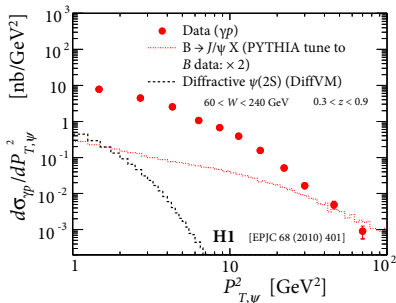
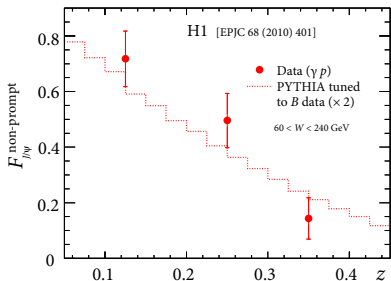
- **b FD** (5% on the  $P_T$ -integrated yields and can go up to  $\approx 50\%$  at  $P_T = 10$  GeV): we do not include it as it can be experimentally removed.

# Feed down

J.P. Lansberg, Phys.Rept. 889 (2020); C.Flore, JP Lansberg, H.S. Shao, YY, PLB 811 (2020) 135926



- **b FD** (5% on the  $P_T$ -integrated yields and can go up to  $\approx 50\%$  at  $P_T = 10$  GeV): we do not include it as it can be experimentally removed.
- **$\chi_c$  FD**: no theory or experimental indication that it could be relevant



- **b FD** (5% on the  $P_T$ -integrated yields and can go up to  $\approx 50\%$  at  $P_T = 10$  GeV): we do not include it as it can be experimentally removed.
- $\chi_c$  FD: no theory or experimental indication that it could be relevant
- 20%  $\psi'$  FD: follows from the ratio of the wave functions at the origin and from the  $\psi' \rightarrow J/\psi$  branching:

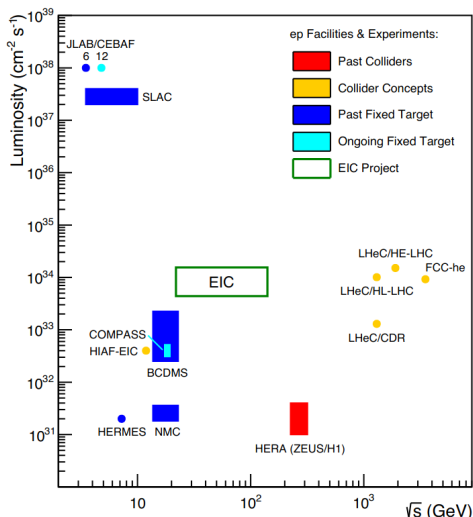
$$FD_{\psi' \rightarrow J/\psi} = |R_{\psi'}(0)|^2 / |R_{J/\psi}(0)|^2 Br(\psi' \rightarrow J/\psi)$$

# Part III

## Photoproduction at mid and high $P_T$ at the Electron-Ion Collider

# The Electron Ion Collider at BNL

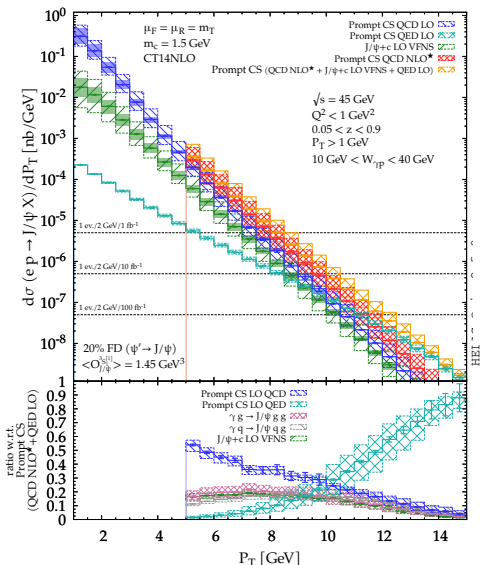
Abhay Deshpande EIC @ BNL, HiX at Kolympari



- Hadrons up to 275 GeV
- Electrons up to 5-10(20) GeV
- CoM  $\sqrt{s}$ : 20-100 (140) GeV
- High luminosity  
 $L_{ep} \propto 10^{33-34} \text{ cm}^{-2} \text{ sec}^{-1}$   
 (100-1000 times HERA)
- World's first:
  - ▶ collider with polarized (min 70%) lepton & proton/light-ion beams
  - ▶ electron-Nucleus collider

# Predictions for the EIC : $J/\psi + X$ ( $\sqrt{s_{ep}} = 45$ GeV)

C.Flore, JP Lansberg, H.S. Shao, YY, PLB 811 (2020) 135926

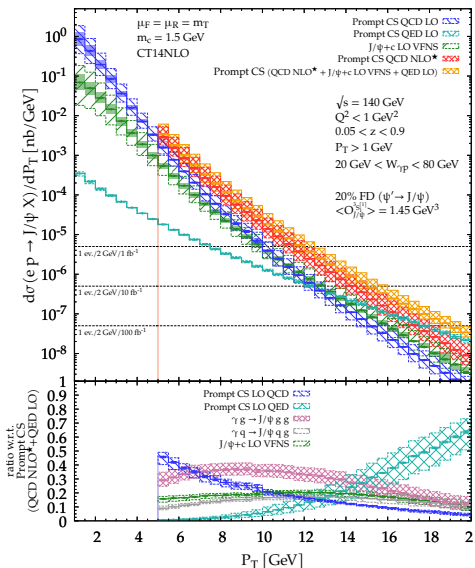


- At  $\sqrt{s_{ep}} = 45$  GeV, one gets into **valence region**
- Yield steeply falling with  $P_T$
- Yield can be measured **up to  $P_T \sim 11$  GeV** with  $\mathcal{L} = 100$  fb<sup>-1</sup>  
[using both  $ee$  and  $\mu\mu$  decay channels and  $\varepsilon_{J/\psi} \simeq 80\%$ ]
- QED contribution leading** at the largest reachable  $P_T$
- photon-quark fusion** contributes more than 30 % for  $P_T > 8$  GeV



# Predictions for the EIC : $J/\psi + X$ ( $\sqrt{s_{ep}} = 140$ GeV)

C.Flore, JP Lansberg, H.S. Shao, YY, PLB 811 (2020) 135926



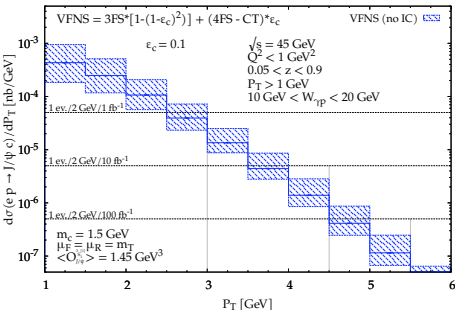
- At  $\sqrt{s_{ep}} = 140$  GeV, larger  $P_T$  range up to approx. 18 GeV
- QED contribution also leading at the largest reachable  $P_T$
- photon-gluon fusion contributions dominant up to approx. 15 GeV
- $J/\psi + 2$  hard partons [*i.e.*  $J/\psi + \{gg, qg, c\bar{c}\}$ ] dominant for  $P_T \sim 8 - 15$  GeV
- It could lead to the observation of  $J/\psi + 2$  jets with moderate  $P_T^{\text{jet}}$
- with a specific topology where the leading  $\text{jet}_1$  recoils on the  $J/\psi + \text{jet}_2$  pair
- We expect the  $d\sigma$  to vanish when  $E_{\text{jet}_2}^{J/\psi \text{ rest fr.}} \rightarrow 0$

# Part IV

## $J/\psi$ +charm associated production at the EIC

# $J/\psi$ +charm associated production at the EIC

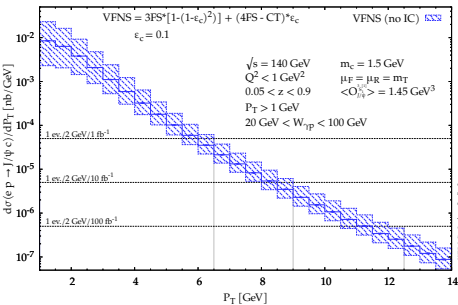
C.Flore, JP Lansberg, H.S. Shao, YY, PLB 811 (2020) 135926



- Same LO VFNS computation previously shown in green except for the **charm-detection efficiency**  
 $\epsilon_C: \sigma^{VFNS} = \sigma^{3FS} \times (1 - (1 - \epsilon)^2) + (\sigma^{4FS} - \sigma^{CT}) \times \epsilon$
- At  $\sqrt{s_{ep}} = 45$  GeV, yield limited to **low  $P_T$**  even with  $\mathcal{L} = 100 \text{ fb}^{-1}$
- But it is clearly observable if  $\epsilon_C = 0.1$  with  $\mathcal{O}(500, 50, 5)$  **events** for  $\mathcal{L} = (100, 10, 1) \text{ fb}^{-1}$

# $J/\psi$ + charm associated production at the EIC

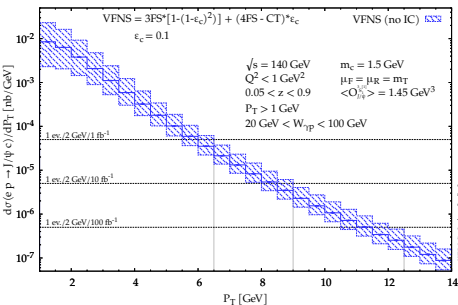
C.Flore, JP Lansberg, H.S. Shao, YY, PLB 811 (2020) 135926



- Same LO VFNS computation previously shown in green except for the **charm-detection efficiency**
- $\epsilon_C: \sigma^{VFNS} = \sigma^{3FS} \times (1 - (1 - \epsilon)^2) + (\sigma^{4FS} - \sigma^{CT}) \times \epsilon$
- At  $\sqrt{s_{ep}} = 45 \text{ GeV}$ , yield limited to **low  $P_T$**  even with  $\mathcal{L} = 100 \text{ fb}^{-1}$
- But it is clearly observable if  $\epsilon_C = 0.1$  with  $\mathcal{O}(500, 50, 5)$  **events for  $\mathcal{L} = (100, 10, 1) \text{ fb}^{-1}$**
- At  $\sqrt{s_{ep}} = 140 \text{ GeV}$ ,  $P_T$  range up to 10 GeV with **up to thousands of events with  $\mathcal{L} = 100 \text{ fb}^{-1}$**
- Could be observed via **charm jet**

# $J/\psi + \text{charm}$ associated production at the EIC

C.Flore, JP Lansberg, H.S. Shao, YY, PLB 811 (2020) 135926

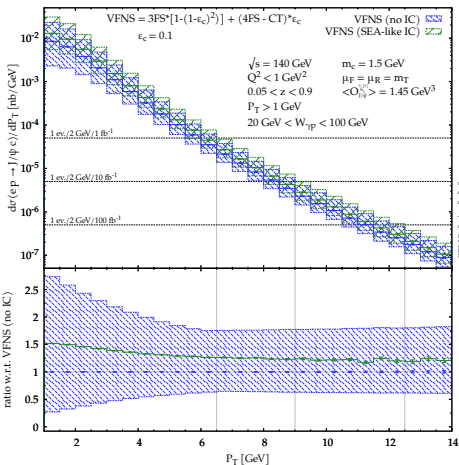


- Same LO VFNS computation previously shown in green except for the **charm-detection efficiency**
- $\epsilon_C: \sigma^{VFNS} = \sigma^{3FS} \times (1 - (1 - \epsilon)^2) + (\sigma^{4FS} - \sigma^{CT}) \times \epsilon$
- At  $\sqrt{s_{ep}} = 45 \text{ GeV}$ , yield limited to **low  $P_T$**  even with  $\mathcal{L} = 100 \text{ fb}^{-1}$
- But it is clearly observable if  $\epsilon_C = 0.1$  with  $\mathcal{O}(500, 50, 5)$  **events for  $\mathcal{L} = (100, 10, 1) \text{ fb}^{-1}$**
- At  $\sqrt{s_{ep}} = 140 \text{ GeV}$ ,  $P_T$  range up to 10 GeV with **up to thousands of events with  $\mathcal{L} = 100 \text{ fb}^{-1}$**
- Could be observed via **charm jet**

- 4FS  $\gamma c \rightarrow J/\psi c$  depend on  $c(x)$  and could be enhanced by **intrinsic charm**

# $J/\psi$ +charm associated production at the EIC

C.Flore, JP Lansberg, H.S. Shao, YY, PLB 811 (2020) 135926

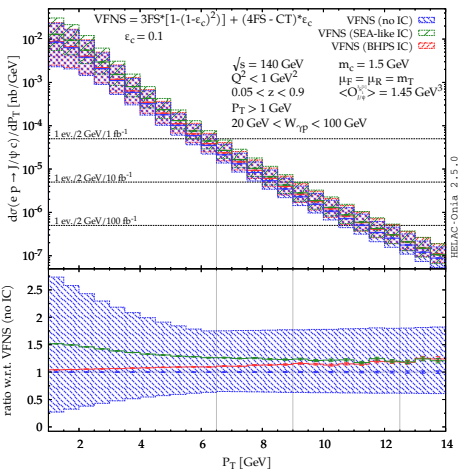


- Same LO VFNS computation previously shown in green except for the **charm-detection efficiency**
- $\epsilon_c: \sigma^{VFNS} = \sigma^{3FS} \times (1 - (1 - \epsilon)^2) + (\sigma^{4FS} - \sigma^{CT}) \times \epsilon$
- At  $\sqrt{s_{ep}} = 45 \text{ GeV}$ , yield limited to **low  $P_T$**  even with  $\mathcal{L} = 100 \text{ fb}^{-1}$
- But it is clearly observable if  $\epsilon_c = 0.1$  with  $\mathcal{O}(500, 50, 5)$  events for  $\mathcal{L} = (100, 10, 1) \text{ fb}^{-1}$
- At  $\sqrt{s_{ep}} = 140 \text{ GeV}$ ,  $P_T$  range up to 10 GeV with **up to thousands of events** with  $\mathcal{L} = 100 \text{ fb}^{-1}$
- Could be observed via **charm jet**

- 4FS  $\gamma c \rightarrow J/\psi c$  depend on  $c(x)$  and could be enhanced by **intrinsic charm**
- Small effect at  $\sqrt{s_{ep}} = 140 \text{ GeV}$  [We used IC  $c(x)$  encoded in CT14NNLO]

# $J/\psi$ + charm associated production at the EIC

C.Flore, JP Lansberg, H.S. Shao, YY, PLB 811 (2020) 135926

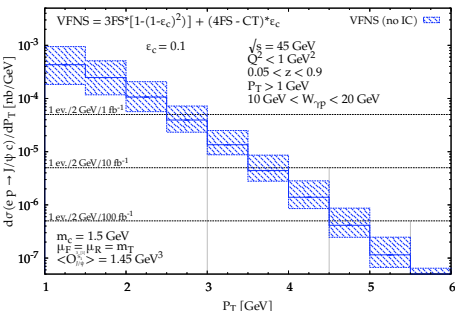


- Same LO VFNS computation previously shown in green except for the **charm-detection efficiency**
- $\epsilon_C$ :  $\sigma^{VFNS} = \sigma^{3FS} \times (1 - (1 - \epsilon)^2) + (\sigma^{4FS} - \sigma^{CT}) \times \epsilon$
- At  $\sqrt{s_{ep}} = 45$  GeV, yield limited to **low  $P_T$**  even with  $\mathcal{L} = 100 \text{ fb}^{-1}$
- But it is clearly observable if  $\epsilon_C = 0.1$  with  $\mathcal{O}(500, 50, 5)$  events for  $\mathcal{L} = (100, 10, 1) \text{ fb}^{-1}$
- At  $\sqrt{s_{ep}} = 140$  GeV,  $P_T$  range up to 10 GeV with **up to thousands of events** with  $\mathcal{L} = 100 \text{ fb}^{-1}$
- Could be observed via **charm jet**

- 4FS  $\gamma c \rightarrow J/\psi c$  depend on  $c(x)$  and could be enhanced by **intrinsic charm**
- Small effect at  $\sqrt{s_{ep}} = 140$  GeV [We used IC  $c(x)$  encoded in CT14NNLO]

# $J/\psi$ + charm associated production at the EIC

C.Flore, JP Lansberg, H.S. Shao, YY, PLB 811 (2020) 135926



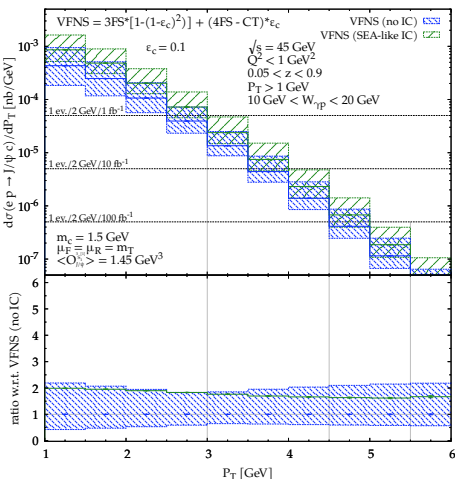
- Same LO VFNS computation previously shown in green except for the **charm-detection efficiency**  
 $\epsilon_C: \sigma^{VFNS} = \sigma^{3FS} \times (1 - (1 - \epsilon)^2) + (\sigma^{4FS} - \sigma^{CT}) \times \epsilon$
- At  $\sqrt{s_{ep}} = 45$  GeV, yield limited to **low  $P_T$**  even with  $\mathcal{L} = 100 \text{ fb}^{-1}$
- But it is clearly observable if  $\epsilon_C = 0.1$  with  $\mathcal{O}(500, 50, 5)$  events for  $\mathcal{L} = (100, 10, 1) \text{ fb}^{-1}$
- At  $\sqrt{s_{ep}} = 140$  GeV,  $P_T$  range up to 10 GeV with **up to thousands of events** with  $\mathcal{L} = 100 \text{ fb}^{-1}$
- Could be observed via **charm jet**

- 4FS  $\gamma c \rightarrow J/\psi c$  depend on  $c(x)$  and could be enhanced by **intrinsic charm**
- Small effect at  $\sqrt{s_{ep}} = 140$  GeV [We used IC  $c(x)$  encoded in CT14NNLO]
- Measurable effect at  $\sqrt{s_{ep}} = 45$  GeV



# $J/\psi$ + charm associated production at the EIC

C.Flore, JP Lansberg, H.S. Shao, YY, PLB 811 (2020) 135926

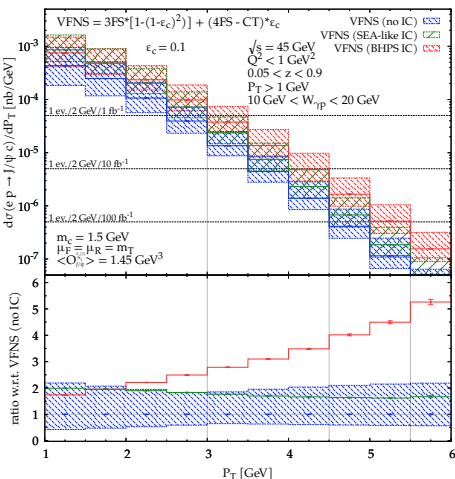


- Same LO VFNS computation previously shown in green except for the **charm-detection efficiency**  
 $\epsilon_c: \sigma^{VFNS} = \sigma^{3FS} \times (1 - (1 - \epsilon)^2) + (\sigma^{4FS} - \sigma^{CT}) \times \epsilon$
- At  $\sqrt{s_{ep}} = 45 \text{ GeV}$ , yield limited to **low  $P_T$**  even with  $\mathcal{L} = 100 \text{ fb}^{-1}$
- But it is clearly observable if  $\epsilon_c = 0.1$  with  $\mathcal{O}(500, 50, 5)$  events for  $\mathcal{L} = (100, 10, 1) \text{ fb}^{-1}$
- At  $\sqrt{s_{ep}} = 140 \text{ GeV}$ ,  $P_T$  range up to 10 GeV with **up to thousands of events** with  $\mathcal{L} = 100 \text{ fb}^{-1}$
- Could be observed via **charm jet**

- 4FS  $\gamma c \rightarrow J/\psi c$  depend on  $c(x)$  and could be enhanced by **intrinsic charm**
- Small effect at  $\sqrt{s_{ep}} = 140 \text{ GeV}$  [We used IC  $c(x)$  encoded in CT14NNLO]
- Measurable effect at  $\sqrt{s_{ep}} = 45 \text{ GeV}$

# $J/\psi$ + charm associated production at the EIC

C.Flore, JP Lansberg, H.S. Shao, YY, PLB 811 (2020) 135926



- Same LO VFNS computation previously shown in green except for the **charm-detection efficiency**  
 $\epsilon_c: \sigma^{VFNS} = \sigma^{3FS} \times (1 - (1 - \epsilon)^2) + (\sigma^{4FS} - \sigma^{CT}) \times \epsilon$
- At  $\sqrt{s_{ep}} = 45 \text{ GeV}$ , yield limited to **low  $P_T$**  even with  $\mathcal{L} = 100 \text{ fb}^{-1}$
- But it is clearly observable if  $\epsilon_c = 0.1$  with  $\mathcal{O}(500, 50, 5)$  events for  $\mathcal{L} = (100, 10, 1) \text{ fb}^{-1}$
- At  $\sqrt{s_{ep}} = 140 \text{ GeV}$ ,  $P_T$  range up to 10 GeV with **up to thousands of events** with  $\mathcal{L} = 100 \text{ fb}^{-1}$
- Could be observed via **charm jet**

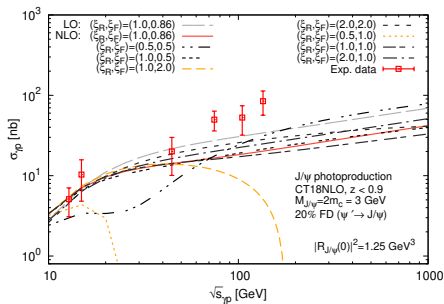
- 4FS  $\gamma c \rightarrow J/\psi c$  depend on  $c(x)$  and could be enhanced by **intrinsic charm**
- Small effect at  $\sqrt{s_{ep}} = 140 \text{ GeV}$  [We used IC  $c(x)$  encoded in CT14NNLO]
- Measurable effect at  $\sqrt{s_{ep}} = 45 \text{ GeV}$ : **BHPS valence-like peak visible!**

# Part V

Study of the impact of the NLO  
corrections to  $P_T$ -integrated  
photoproduction cross section

# The negative cross-sections issue at high energies

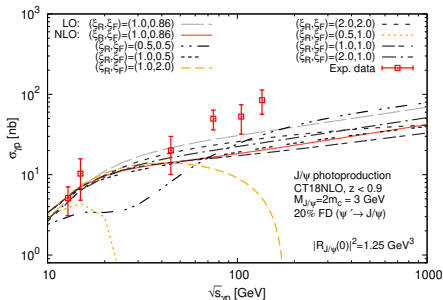
A. Colpani Serri, Y. Feng, C. Flore, J.P. Lansberg, M.A. Ozcelik, H.S. Shao, YY: arXiv:2112.05060 [hep-ph]



Exp. data: H1 - M.Kraemer: NPB 459(1996)3-50, FTPS - B.H.Denby et al.: PRL 52(1984)795-798, NAI - NA14Collaboration, R.Barate et al.:Z.Phys.C 33(1987)505

# The negative cross-sections issue at high energies

A. Colpani Serri, Y. Feng, C. Flore, J.P. Lansberg, M.A. Ozelik, H.S. Shao, YY: arXiv:2112.05060 [hep-ph]

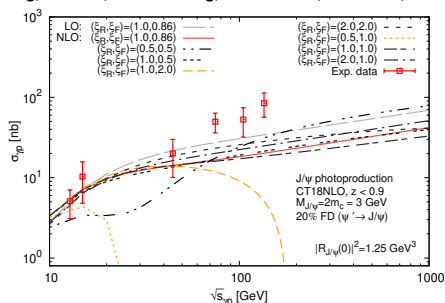


- **NLO** cross section for  $J/\psi$  photoproduction becomes negative for **large**  $\mu_F$  when  $\sqrt{s_{\gamma p}}$  increases

Exp. data: H1 - M.Kraemer: NPB 459(1996)3-50, FTPS - B.H.Denby et al.: PRL 52(1984)795-798, NAI - NA14Collaboration, R.Barate et al.:Z.Phys.C 33(1987)505

# The negative cross-sections issue at high energies

A. Colpani Serri, Y. Feng, C. Flore, J.P. Lansberg, M.A. Ozelik, H.S. Shao, YY: arXiv:2112.05060 [hep-ph]



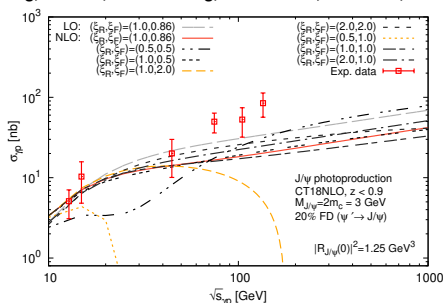
- **NLO** cross section for  $J/\psi$  photoproduction becomes negative for **large**  $\mu_F$  when  $\sqrt{s_{\gamma p}}$  increases
- For  $\mu_F = 2M$ ,  $\sigma < 0$  as in case of  $\eta_c$  hadroproduction

J.P. Lansberg, M.A. Ozelik: Eur.Phys.J.C 81 (2021) 6, 497

Exp. data: H1 - M.Kraemer: NPB 459(1996)3-50, FTPS - B.H.Denby et al.: PRL 52(1984)795-798, NAI - NA14Collaboration, R.Barate et al.:Z.Phys.C 33(1987)505

# The negative cross-sections issue at high energies

A. Colpani Serri, Y. Feng, C. Flore, J.P. Lansberg, M.A. Ozelik, H.S. Shao, YY: arXiv:2112.05060 [hep-ph]



- **NLO** cross section for  $J/\psi$  photoproduction becomes negative for **large**  $\mu_F$  when  $\sqrt{s_{\gamma p}}$  increases
- For  $\mu_F = 2M$ ,  $\sigma < 0$  as in case of  $\eta_c$  hadroproduction

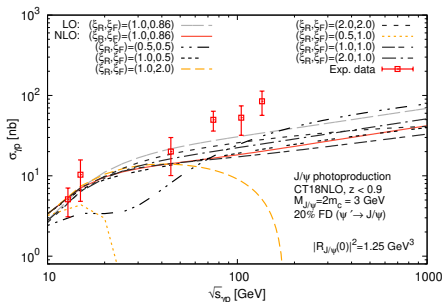
J.P. Lansberg, M.A. Ozelik: Eur.Phys.J.C 81 (2021) 6, 497

- 2 possible sources of negative partonic cross sections: loop corrections (interference) and from real emission (subtraction of IR poles)

Exp. data: H1 - M.Kraemer: NPB 459(1996)3-50, FTPS - B.H.Denby et al.: PRL 52(1984)795-798, NAI - NA14Collaboration, R.Barate et al.:Z.Phys.C 33(1987)505

# Negative cross-section values

A. Colpani Serri, Y. Feng, C. Flore, J.P. Lansberg, M.A. Ozelcik, H.S. Shao, YY: arXiv:2112.05060 [hep-ph]

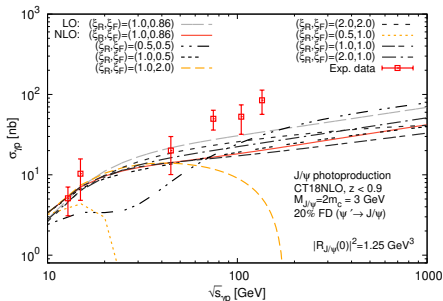


- Initial state collinear divergences are removed via the **subtraction** into the PDFs via AP-CT



# Negative cross-section values

A. Colpani Serri, Y. Feng, C. Flore, J.P. Lansberg, M.A. Ozelcik, H.S. Shao, YY: arXiv:2112.05060 [hep-ph]

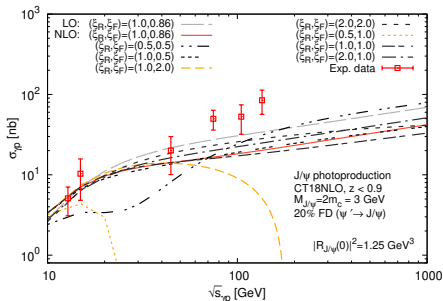


- Initial state collinear divergences are removed via the **subtraction** into the PDFs via AP-CT

- $$\lim_{\hat{s} \rightarrow \infty} \hat{\sigma}_{\gamma i}^{NLO} \propto \left( \log \frac{M_Q^2}{\mu_F^2} + A_{\gamma i} \right), \quad A_{\gamma g} = A_{\gamma q}$$

# Negative cross-section values

A. Colpani Serri, Y. Feng, C. Flore, J.P. Lansberg, M.A. Ozelcik, H.S. Shao, YY: arXiv:2112.05060 [hep-ph]

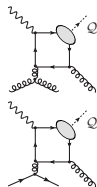


- Initial state collinear divergences are removed via the **subtraction** into the PDFs via AP-CT
- $\lim_{\hat{s} \rightarrow \infty} \hat{\sigma}_{\gamma i}^{NLO} \propto \left( \log \frac{M_Q^2}{\mu_F^2} + A_{\gamma i} \right), A_{\gamma g} = A_{\gamma q}$
- If large  $\mu_F \rightarrow \hat{\sigma} < 0 \rightarrow \sigma < 0$ : over-subtraction from AP-CT into the PDFs

# A scale prescription for $\mu_F$

J.P. Lansberg, M.A. Ozelik: Eur.Phys.J.C 81 (2021) 6, 497

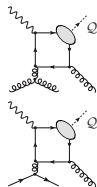
- In principle, such negative terms should be compensated by the **evolution** of the PDFs governed by the DGLAP equations;



# A scale prescription for $\mu_F$

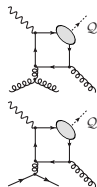
J.P. Lansberg, M.A. Ozelik: Eur.Phys.J.C 81 (2021) 6, 497

- In principle, such negative terms should be compensated by the **evolution** of the PDFs governed by the DGLAP equations;
- $A_{\gamma g}, A_{\gamma q}$  are **process-dependent**, while the DGLAP equations are **process-independent**, which makes the compensation imperfect;



# A scale prescription for $\mu_F$

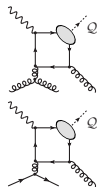
J.P. Lansberg, M.A. Ozelik: Eur.Phys.J.C 81 (2021) 6, 497



- In principle, such negative terms should be compensated by the **evolution** of the PDFs governed by the DGLAP equations;
- $A_{\gamma g}, A_{\gamma q}$  are **process-dependent**, while the DGLAP equations are **process-independent**, which makes the compensation imperfect;
- But as  $A_{\gamma g} = A_{\gamma q}$ , we can **choose**  $\mu_F$  such that  $\lim_{\hat{s} \rightarrow \infty} \hat{\sigma}_{\gamma i}^{NLO} = 0$

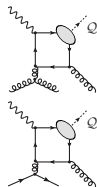
# A scale prescription for $\mu_F$

J.P. Lansberg, M.A. Ozelik: Eur.Phys.J.C 81 (2021) 6, 497



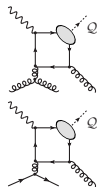
- In principle, such negative terms should be compensated by the **evolution** of the PDFs governed by the DGLAP equations;
- $A_{\gamma g}, A_{\gamma q}$  are **process-dependent**, while the DGLAP equations are **process-independent**, which makes the compensation imperfect;
- But as  $A_{\gamma g} = A_{\gamma q}$ , we can **choose**  $\mu_F$  such that  $\lim_{\hat{s} \rightarrow \infty} \hat{\sigma}_{\gamma i}^{NLO} = 0$
- This amounts to consider that all the QCD corrections are in the PDFs

# A scale prescription for $\mu_F$



- In principle, such negative terms should be compensated by the **evolution** of the PDFs governed by the DGLAP equations;
- $A_{\gamma g}, A_{\gamma q}$  are **process-dependent**, while the DGLAP equations are **process-independent**, which makes the compensation imperfect;
- But as  $A_{\gamma g} = A_{\gamma q}$ , we can **choose**  $\mu_F$  such that  $\lim_{\hat{s} \rightarrow \infty} \hat{\sigma}_{\gamma i}^{NLO} = 0$
- This amounts to consider that all the QCD corrections are in the PDFs
- The choice of factorisation scale to avoid possible negative hadronic cross-section: (for  $\eta_Q : A_{gi} = -1$ )  
 $\mu_F = \hat{\mu}_F = M e^{A_{\gamma i}/2};$

# A scale prescription for $\mu_F$



- In principle, such negative terms should be compensated by the **evolution** of the PDFs governed by the DGLAP equations;
- $A_{\gamma g}, A_{\gamma q}$  are **process-dependent**, while the DGLAP equations are **process-independent**, which makes the compensation imperfect;
- But as  $A_{\gamma g} = A_{\gamma q}$ , we can **choose**  $\mu_F$  such that  $\lim_{\hat{s} \rightarrow \infty} \hat{\sigma}_{\gamma i}^{NLO} = 0$
- This amounts to consider that all the QCD corrections are in the PDFs
- The choice of factorisation scale to avoid possible negative hadronic cross-section: (for  $\eta_Q$  :  $A_{gi} = -1$ )  
 $\mu_F = \hat{\mu}_F = M e^{A_{\gamma i}/2}$ ;
- For  $J/\psi$  ( $Y$ ) photoproduction:  $\hat{\mu}_F = 0.86M$   
( $P_T \in [0, \infty]$ ,  $z < 0.9$ )



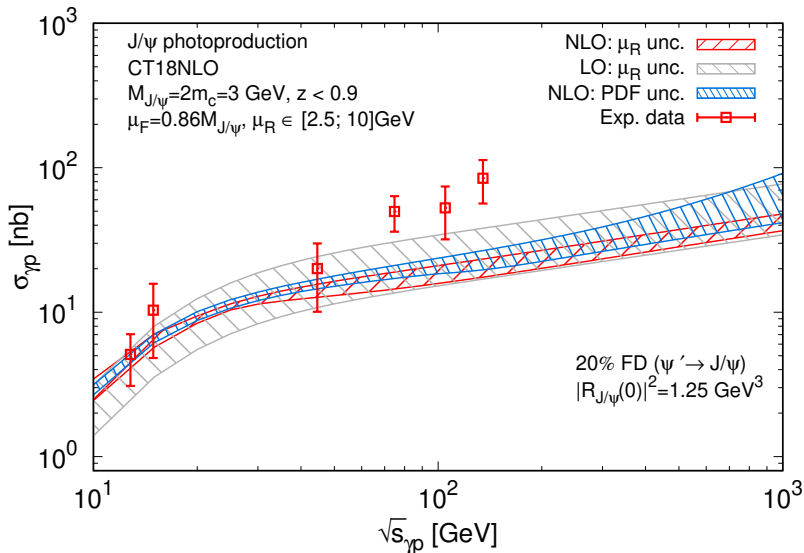
# HEF: resummation of collinear emission contributions

J.P. Lansberg, M.Nefedov, M.A. Ozcelik: 2112.06789 [hep-ph]

- Mellin transformation:  $f(N) = \int_0^1 dx x^{N-1} f(x)$ , we can rewrite  $\hat{\sigma}$  from  $x$  to  $N$  space
- From the DGLAP equations we know that:  
 $f(N, \hat{\mu}_F) \approx f(N, \mu_0) \exp\left(\frac{2A\alpha_s(\mu_0)C_A}{\pi N}\right)$ , where we used  $\gamma_{gg}(N) \approx \frac{2C_A}{N}$ ;  $\alpha_s \neq \alpha_s(\mu)$ ,  $\mu_0$  is the default scale choice.
- In the exponent we did some approximate resummation of collinear emission contributions for  $\hat{s} \rightarrow \infty$ :  
 $\alpha_s^n \ln^{n-1} \frac{1}{\hat{z}} \rightarrow \frac{\alpha_s^n}{N^n}$  for  $n = 0$ , where  $\hat{z} = \frac{M^2}{\hat{s}}$

# Results with $\hat{\mu}_F = 0.85M$

A. Colpani Serri, Y. Feng, C. Flore, J.P. Lansberg, M.A. Ozcelik, H.S. Shao, YY: arXiv:2112.05060 [hep-ph]



Exp. data: H1 - M.Kraemer: Nucl.Phys.B 459(1996)3-50, FTPS - B.H.Denbyet al.: Phys.Rev.Lett. 52(1984)795-798, NAI - NA14Collaboration, R.Barateet al.:Z.Phys.C 33(1987)505

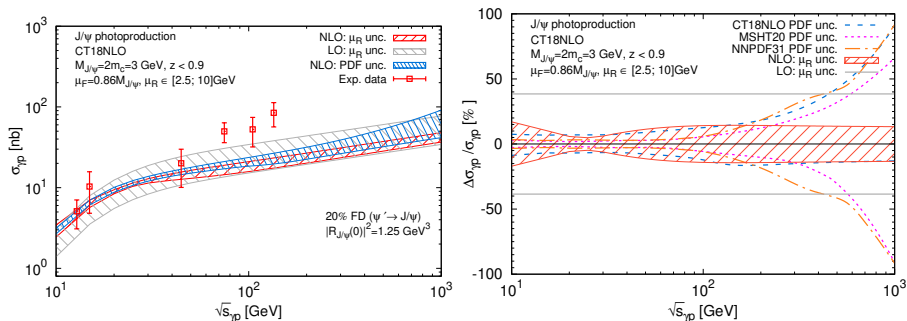
## Part VI

Can  $J/\psi$  &  $\Upsilon$  allow us to probe PDFs? :  
PDF vs scale uncertainties

# $J/\psi$ : PDF uncertainties of $\sigma(\sqrt{s_{\gamma p}})$

A. Colpani Serri, Y. Feng, C. Flore, J.P. Lansberg, M.A. Ozcelik, H.S. Shao, YY: arXiv:2112.05060 [hep-ph]

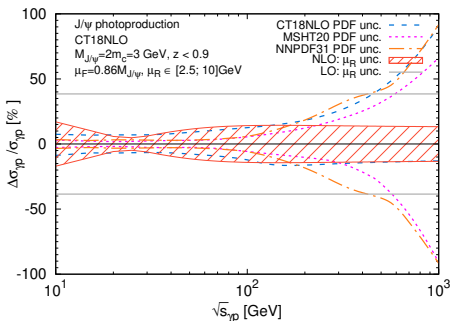
- PDF uncertainties increase at large  $\sqrt{s}$  (i.e. small  $x$ )
- The  $\mu_R$  unc. are reduced at NLO in comparison with LO;



# $J/\psi$ : PDF uncertainties of $\sigma(\sqrt{s_{\gamma p}})$

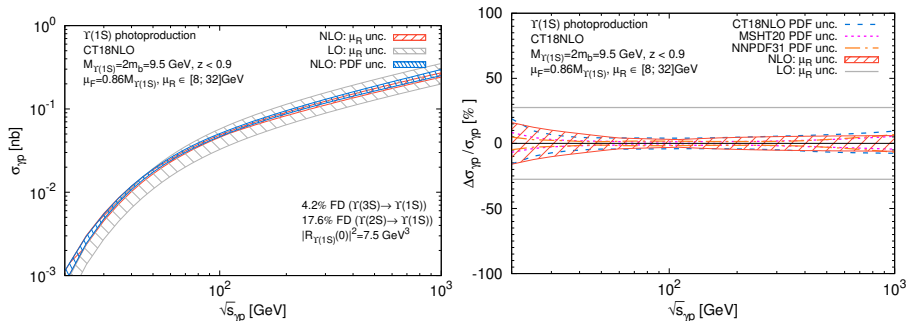
A. Colpani Serri, Y. Feng, C. Flore, J.P. Lansberg, M.A. Ozcelik, H.S. Shao, YY: arXiv:2112.05060 [hep-ph]

- PDF uncertainties increase at large  $\sqrt{s}$  (i.e. small  $x$ )
- The  $\mu_R$  unc. are reduced at NLO in comparison with LO;
- An increase of  $\mu_R$  unc. from  $\sqrt{s_{\gamma p}} \gtrsim 50$  GeV comes from the loop corrections.
- At NNLO we will have such contributions squared; we expect rather positive NNLO corrections, which will reduce  $\mu_R$  unc.



# $\Upsilon$ photoproduction

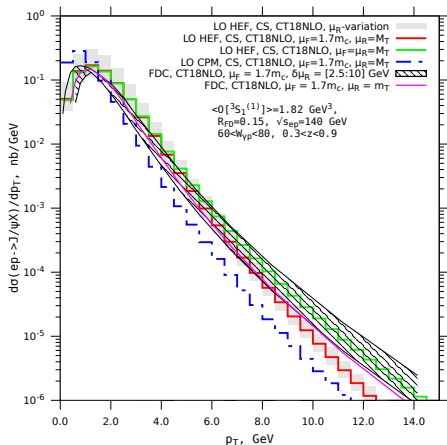
A. Colpani Serri, Y. Feng, C. Flore, J.P. Lansberg, M.A. Ozcelik, H.S. Shao, YY: arXiv:2112.05060 [hep-ph]



- We see further reduction of scale uncertainties at NLO comparably to LO
- PDF uncertainties are larger at high  $\sqrt{s_{\gamma p}}$ : a potential to probe PDFs

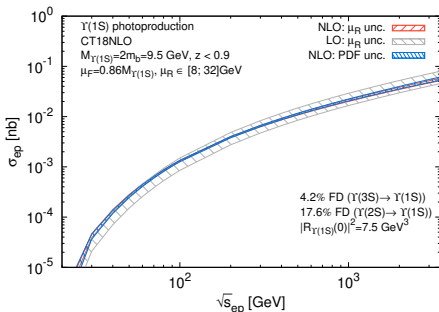
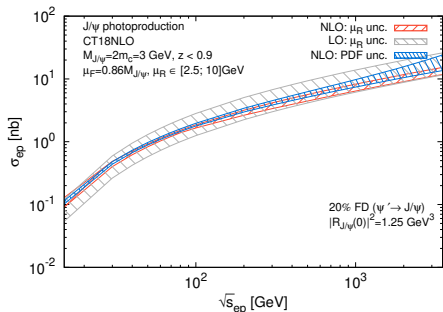
# Predictions of the high-energy factorization

a private communication with M.Nefedov;



- The Leading-Twist High-Energy factorization (HEF) is the formalism to resum large logarithms  $\ln(1/z_+)$  in higher-order corrections to the CF description of inclusive  $l-h$  &  $h-h$  reactions
- No significant difference with NLO at low  $p_T$
- **However**, at large  $P_T$  HEF may be not applicable
- We need a consistent matching with NLO CF calculation

NB:  $z_+ = p_J^+ / (x_1 P^+)$ : LC  $k^\pm = k^0 \pm k^3$ ,  $x_1$  is the momentum fraction of the parton initiating the hard process,  $P^+ = 2E_p - (+)$ -comp. of p moment.



Exp.	$\sqrt{s_{ep}}$	$\mathcal{L} \text{ (fb}^{-1}\text{)}$	$N_{J/\psi}$	$N_{Y(1S)}$
EIC	45	100	$8.5^{+0.5}_{-1.0} \cdot 10^6$	$7.8^{+0.9}_{-1.1} \cdot 10^2$
EIC	140	100	$2.5^{+0.1}_{-0.4} \cdot 10^7$	$9.7^{+0.3}_{-0.9} \cdot 10^3$

$$N_{\psi'} \simeq 0.08 \times N_{J/\psi},$$

$$N_{Y(2S)} \simeq 0.5 \times N_{Y(1S)},$$

$$N_{Y(3S)} \simeq 0.4 \times N_{Y(1S)}$$

We expect  $\mu_R$  unc. to shrink at NNLO: possibility to constrain PDF



# Part VII

## Electroproduction of $J/\psi$ and $\Upsilon$

# Inclusive electroproduction

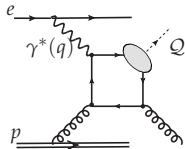
J.P. Lansberg, Phys.Rept. 889 (2020); Z. Sun, H.F. Zhang, Phys.Rev.D 96 (2017) 9, 091502; J.W. Qiu, X.P. Wang, H. Xing, Chin.Phys.Lett. 38 (2021) 4, 041201

- Inclusive  $J/\psi(\Upsilon)$  production:

$$\gamma(Q^2 > Q_0^2) + p \rightarrow J/\psi + X;$$

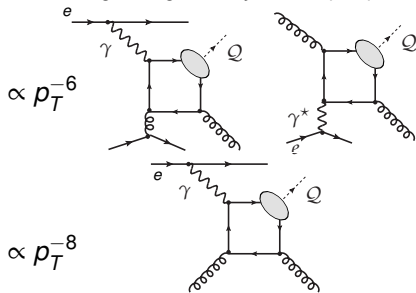
for  $Q_0^2 \approx (1, 1.5)\text{GeV}^2$

- Small resolved contributions
- Larger  $Q^2$  (higher resolution) **suppress the gluon saturation effects and also improve the perturbative expansion in  $\alpha_s$**
- The computation **more complicated**
- $\sigma$  **is suppressed  $1/Q^4$** ; only 4 exp. studies: H1 (Eur.Phys.J.C 10 (1999), 373-393); Eur.Phys.J.C 25 (2002), 41-53; Eur.Phys.J.C 68 (2010), 401-420), **ZEUS** (Eur.Phys.J.C 44 (2005), 13-25)



# Photoproduction vs electroproduction of $J/\psi$

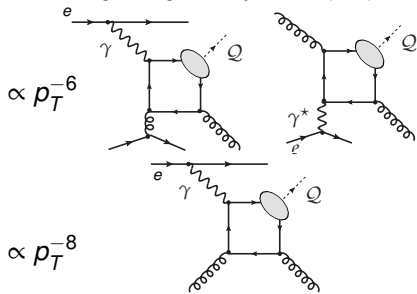
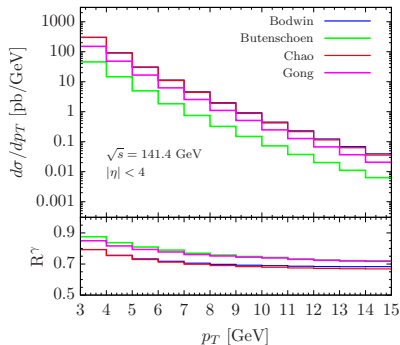
J.W. Qiu, X.P. Wang, H. Xing, Chin.Phys.Lett. 38 (2021) 4, 041201



- The electroproduction could scale as  $\propto p_T^{-6}$  and the photoproduction as  $\propto p_T^{-8}$

# Photoproduction vs electroproduction of $J/\psi$

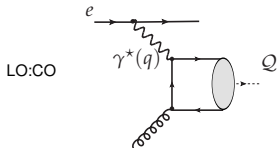
J.W. Qiu, X.P. Wang, H. Xing, Chin.Phys.Lett. 38 (2021) 4, 041201



- The electroproduction could scale as  $\propto p_T^{-6}$  and the photoproduction as  $\propto p_T^{-8}$
- $R^\gamma = 1$ : only photoproduction;  $R^\gamma = 0$ : only electroproduction
- So, at higher  $p_T$  the effect for electroproduction will be larger

# LDME study with electroproduction of $J/\psi$

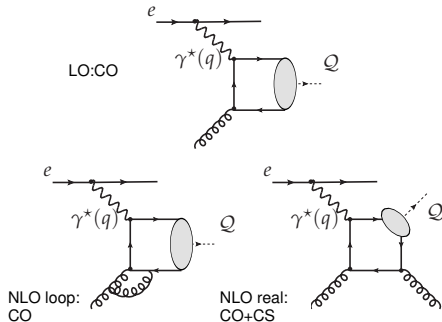
J.W. Qiu, X.P. Wang, H. Xing, Chin.Phys.Lett.38 (2021) 4, 041201



- At LO only color octet  $^1S_0^{[8]}$  and  $^3P_J^{[8]}$   $c\bar{c}$  pair can contribute to high  $p_T$   $J/\psi$  production in  $ep$  collisions

# LDME study with electroproduction of $J/\psi$

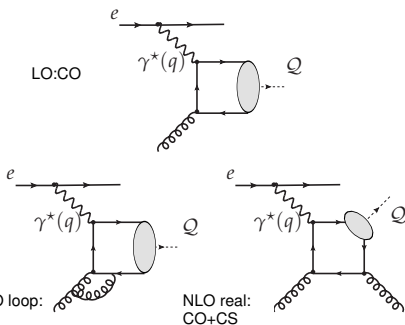
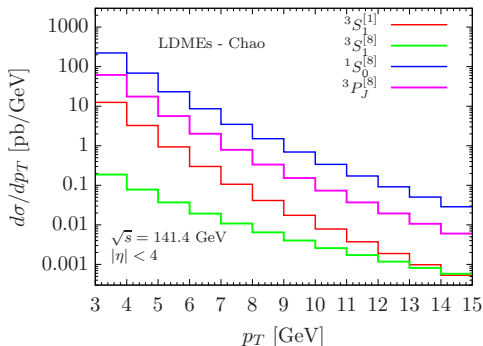
J.W. Qiu, X.P. Wang, H. Xing, Chin.Phys.Lett.38 (2021) 4, 041201



- At LO only color octet  $^1S_0^{[8]}$  and  $^3P_J^{[8]}$   $c\bar{c}$  pair can contribute to high  $p_T$   $J/\psi$  production in  $ep$  collisions
- For NLO real contribution, all four leading  $c\bar{c}$  states ( $^3S_1^{[1]}$ ,  $^1S_0^{[8]}$ ,  $^3S_1^{[8]}$ ,  $^3P_J^{[8]}$ ) contribute

# LDME study with electroproduction of $J/\psi$

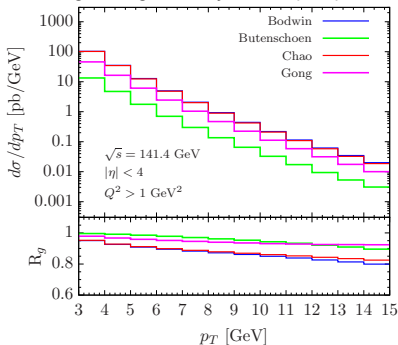
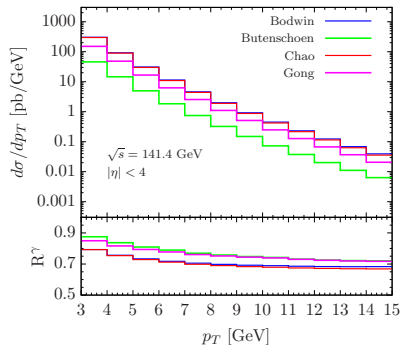
J.W. Qiu, X.P. Wang, H. Xing, Chin.Phys.Lett.38 (2021) 4, 041201



- At LO only color octet  $^1S_0^{[8]}$  and  $^3P_J^{[8]}$   $c\bar{c}$  pair can contribute to high  $p_T$   $J/\psi$  production in  $ep$  collisions
- For NLO real contribution, all four leading  $c\bar{c}$  states ( $^3S_1^{[1]}$ ,  $^1S_0^{[8]}$ ,  $^3S_1^{[8]}$ ,  $^3P_J^{[8]}$ ) contribute
- If  $^1S_0^{[8]}$  dominates, since it is unpolarised, high- $p_T$   $J/\psi$  produced in inclusive  $ep$  collisions are expected to be unpolarized.

# Introducing GeV inclusive electroproduction of $J/\psi$

J.W. Qiu, X.P. Wang, H. Xing, Chin.Phys.Lett.38 (2021) 4, 041201



- Different sets of LDMEs lead to very different production rate  $\rightarrow$  could provide new insights into the  $J/\psi$  production mechanism
- $R_g \rightarrow 1$  (the gluon initiated fraction of total  $d\sigma$ ): the production is dominated by initial gluon channel (as for photoproduction: s.12)  $\rightarrow$  a good observable to probe the initial gluon PDF



# Part VIII

## Conclusions

# Conclusions

- The CSM up to  $\alpha\alpha_s^3$  reproduces photoproduction at HERA
- The EIC predictions can rely on CSM only
- The consistent matching of HEF with NLO CF calculation can improve the photoproduction predictions

# Conclusions

- The CSM up to  $\alpha\alpha_s^3$  reproduces photoproduction at HERA
- The EIC predictions can rely on CSM only
- The consistent matching of HEF with NLO CF calculation can improve the photoproduction predictions
- We have also seen that QCD corrections are important for  $P_T$ -integrated  $\sigma$
- A specific  $\mu_F$  choice can be employed to avoid a possible over subtraction of collinear divergences which lead to NLO negative  $\sigma$  values at large  $\sqrt{s_{\gamma p}}$
- Loop correction matter and significant NNLO corrections (likely positive) are expected as well as a further reduction of the  $\mu_R$  unc., esp. around 100 GeV
- This would likely allow one to better probe gluon PDFs

# Conclusions

- The CSM up to  $\alpha\alpha_s^3$  reproduces photoproduction at HERA
- The EIC predictions can rely on CSM only
- The consistent matching of HEF with NLO CF calculation can improve the photoproduction predictions
- We have also seen that QCD corrections are important for  $P_T$ -integrated  $\sigma$
- A specific  $\mu_F$  choice can be employed to avoid a possible over subtraction of collinear divergences which lead to NLO negative  $\sigma$  values at large  $\sqrt{s_{\gamma p}}$
- Loop correction matter and significant NNLO corrections (likely positive) are expected as well as a further reduction of the  $\mu_R$  unc., esp. around 100 GeV
- This would likely allow one to better probe gluon PDFs
- Inclusive electroproduction of  $J/\psi$  measured at the EIC could allow for new constraints of the gluon PDF over a wide range of scales
- The EIC could provide the 1st measurement of  $\Upsilon$  electroproduction

# Backup

# Feed down

C.Flore, JP Lansberg, H.S. Shao, YY, PLB 811 (2020) 135926

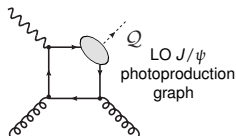
- **b FD** (5% on the  $P_T$ -integrated yields and is significant around  $P_T = 10$  GeV): we do not include it as it can be experimentally removed.
- Tune Pythia 8.2 using a b analysis by H1 using di-electrons events which extends to large  $P_T$ 
  - ▶ Compute the corresponding LO+PS cross section using Pythia 8.2
  - ▶ Perform a  $\chi^2$ -minimisation to compute a tuning factor (absorbs the theory uncertainties), such that the obtained LO+PS Pythia spectrum reproduces best the H1 b data
  - ▶ Again use Pythia 8.2 to compute the  $b \rightarrow J/\psi$  cross section in the H1 kinematics.
  - ▶ Subtract this  $b \rightarrow J/\psi$  yield from the inclusive one
- **$\chi_c$  FD**: no theory or experimental indication that it could be relevant
- **20%  $\psi'$  FD**: follows from the ratio of the wave functions at the origin and from the  $\psi' \rightarrow J/\psi$  branching:  $FD_{\psi' \rightarrow J/\psi} = |R_{\psi'}(0)|^2 / |R_{J/\psi}(0)|^2 Br(\psi' \rightarrow J/\psi)$

# Basic pQCD approach: the Colour Singlet Model (CSM)

C.-H. Chang, NPB172, 425 (1980); R. Baier & R. Rückl Z. Phys. C 19, 251(1983);

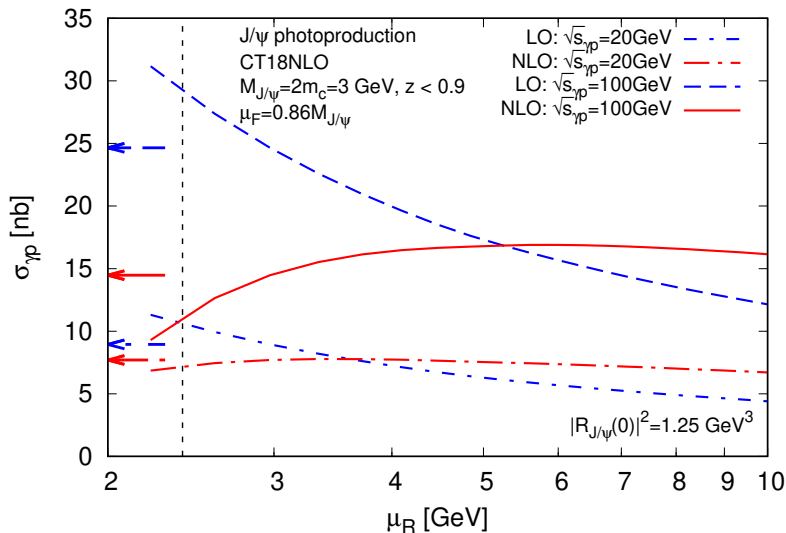
One supposes two **factorisations**:

- 1 **collinear**, in which the hadronic cross section can be written as the convolution of the **PDFs** with the **partonic cross section**;
- 2 between the hard part (a perturbative amplitude, which describes the  $Q\bar{Q}$  **pair production**) and the soft part (a non-perturbative matrix element, which describes **hadronisation**):
  - Perturbative creation of 2 quarks,  $Q$  and  $\bar{Q}$ 
    - ▶ on-shell
    - ▶ in a colour singlet state
    - ▶ with a vanishing relative momentum
    - ▶ in a  $^3S_1$  state (for  $J/\psi$ ,  $\psi'$  and  $\Upsilon$ )
  - Non-perturbative binding of quarks  
→ Schrödinger wave function at  $r = 0$



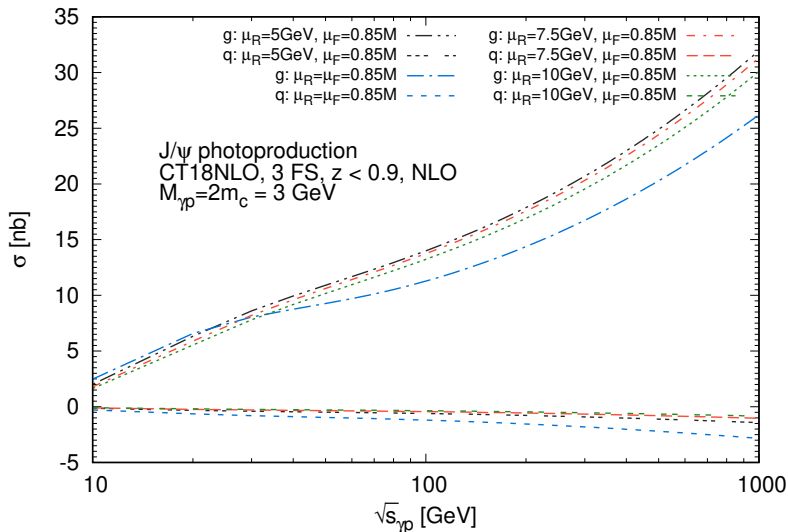
**CSM:** the Taylor series expansion of the amplitude in the  $Q\bar{Q}$  relative momentum ( $v$ ) to the first non-vanishing (Leading- $v$  NRQCD) term.

# Dependence of $\sigma_{\gamma p}$ on the $\mu_R$ at an initial photon energy $s_{\gamma p}$

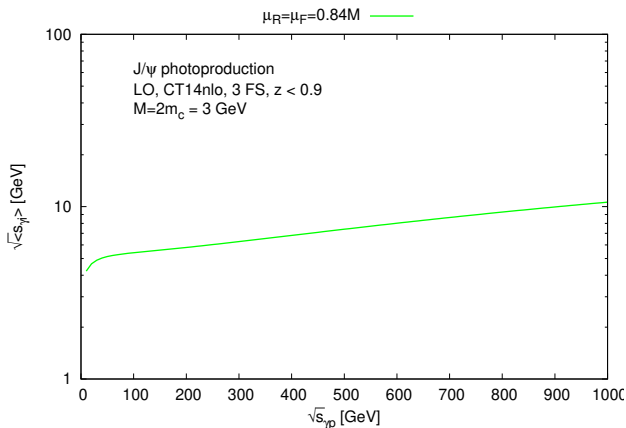




# q& g contributions



# $\mu_R$ choice



- 1 the natural scale choice in case of  $J/\psi$  photoproduction is not a mass of  $c$ -quark, because of some loop corrections.
- 2 For  $J/\psi$ :  
 $\mu_{Rmin} = 1.6m_c$   
( $\sqrt{s_{\gamma p}} = 10\text{GeV}$ )

# NLO\*: $P_T$ -discussion

**IR cut-off** - a lower cut on the invariant mass of each pair of massless partons,  $s_{ij}$ .

$$\ln(s_{ij}^{min})(1/p_T)^N, \quad N \geq 8$$

If the initial gluon/quark emits a large- $p_T$  gluon/quark and if the final gluon is semi-hard, the increase of  $p_T$  results in the growth of all the possible  $s_{ij} \rightarrow (1/p_T)^6$

We do not consider loop corrections in NLO\*:  $(1/p_T)^8$

